Retinoblastoma: Animal Models of Tumor Progression

Patricia Chévez-Barrios[1,2], Mary Y. Hurwitz[3,5], Kathryn Louie[4,5], Karen T. Marcus [3,5], Vien N. Holcombe [3,5], Pamela Schafer[5], C. Estuardo Aguilar-Cordova[3,4,5], and Richard L. Hurwitz[2,5,4,5]

Departments of Pathology[1], Ophthalmology[2], Pediatrics[3],
The Center for Cell and Gene Therapy[4] and The Texas Children's Cancer Center[5];
Baylor College of Medicine, Houston, TX 77030

Number of Text Pages: 13
Number of Tables: 2
Number of Figures: 3

Short title: Animal models of retinoblastoma

Supported by grants from the Lions Eye Bank (PC-B), the Moran Foundation (PC-B), the Knights Templar Eye Foundation, Inc. (MYH), the General Clinical Research Center #M01RR00188 (CEA-C), the Foundation for Research (RLH) and the Retina Research Foundation (RLH)

Corresponding Author and Reprint Requests:

Richard L. Hurwitz
6621 Fannin Street, M.C. 3-3320
Houston, TX 77030
e-mail: rhurwitz@bcm.tmc.edu
phone: (713)770-4260
fax: (713)770-4202

ABSTRACT

To generate animal models of retinoblastoma that closely resemble metastatic and nonmetastatic human disease for the purposes of examining tumor biology and of developing alternate treatments, human retinoblastoma cell lines were injected into the vitreal cavities of immunodeficient mice. Two reproducible animal models with contrasting biologic behavior analogous to human retinoblastoma have been developed. The Y79 retinoblastoma model demonstrated specific tumor progression similar to that seen in human metastatic disease. Y79 retinoblastoma cells formed intraocular tumors that were initially confined to the vitreal cavity. Tumors progressively invaded the retina, subretinal space, choroid and optic nerve head, and anterior chamber of the eye. Tumors progressed into the subarachnoid space and focally invaded the brain and contralateral optic nerve. Large tumors developed extraocular extensions. The histology of the tumors showed a poorly differentiated pattern with high mitotic rate, foci of necrosis, and calcification. The WERI-Rb model more closely resembled non-metastatic human retinoblastoma. WERI- Rb tumors were localized in the eye with only anterior choroidal invasion at late stages. To examine potential biological differences *in vitro*, the retinoblastoma cell lines were co-cultured with adherent choroid cells or adherent glioma cells which represent the targets of metastatic retinoblastoma *in vivo*. Consistent with the *in vivo* observations, Y79 cells but not WERI-Rb cells adhere specifically to both the choroidal and the glioma cell lines.

INTRODUCTION

Retinoblastoma is the most common primary intraocular tumor in children. This disease presents most frequently as unilateral sporadic tumors and less frequently as bilateral hereditary tumors. When left untreated, retinoblastoma is almost always fatal. Prognosis is affected by many risk factors the most important of which is the extent of invasion of the retinoblastoma into ocular coats and the optic nerve (1). When retinoblastoma is adequately treated in the early stages by enucleation, the cure rates approach 95% (2-4). Besides the loss of vision, this therapeutic approach leaves the child with a lasting cosmetic deformity that worsens throughout life (5). In addition there has been no successful therapy for the treatment of patients who develop metastatic disease. Therefore, animal models of retinoblastoma that accurately reproduce the tumors' behaviors are critical for the examination of new approaches to treatment and may also lead to an understanding of the mechanisms of metastases.

Retinoblastoma is a uniquely human disease. Attempts to develop animal models have been complicated by a tendency to form other tumors and by the lack of reproducibility of the invasive behavior observed in human retinoblastoma (6, 7). The majority of the models have been created by injecting retinoblastoma tumor cells into either the anterior chamber or the subretinal space of the eyes of nude mice or rats. Injection of tumor cells into the anterior chamber was favored because of that site's accessibility, both for the injection and for follow up observations (8). Anterior chamber injection of Y79 cells has previously been reported to result in the

invasion of the optic nerve and brain (9). These studies did not attempt to clarify whether the tumor spread by nonspecific direct extension or by specific migration of the tumor through the optic nerve to the central nervous system as is characteristic of human retinoblastoma. Tumor involvement of the anterior chamber is a late occurrence in human disease and the physiological environment of the anterior chamber differs significantly from that of the vitreal cavity (10, 11). Therefore this model would not be useful to study metastatic behavior of the tumor or serve as a model for therapeutic trials. Another animal model in which retinoblastoma cells were injected into the subretinal space more closely resembles human retinoblastoma in location (12, 13). However, injections into the subretinal space disrupt the choroid and the retina, hence studies of invasiveness and of progression of retinoblastoma have been limited. Transgenic mice expressing viral oncogenes under the control of vision-specific promoters (opsin or interphotoreceptor retinoid-binding protein - IRBP) have also been used to study retinoblastoma (6, 7, 14). These mice tended to develop trilateral retinoblastoma shortly after birth with tumor involvement in both eyes and the pineal, a rare occurrence in children. In addition, trilateral involvement complicates the accurate diagnosis of metastasis to the brain.

This paper reports two murine models of intraocular retinoblastoma, one that effectively resembles the histopathologic and biologic behavior of human metastatic disease and the other that mimics nonmetastatic disease.

METHODS

CELL CULTURE: The human retinoblastoma Y79 and WERI- Rb (ATCC HTB 18 and ATCC HTB 169 respectively), the human embryonic kidney HEK293 (ATCC CRL 1573), the rhesus monkey choroidal RF/6A (ATCC CRL 1780), and the human glioma Hs 683 (ATCC HTB 138) cell lines were cultured in GVL Modified Eagle's Minimum Essential Medium supplemented with fetal calf serum (5%; Hyclone), streptomycin (100 μg/ml; Irvine Scientific) and penicillin (100 units/ml; Irvine Scientific). Y79 and WERI-Rb cells were grown in suspension at a concentration of 10^5-10^6 cells/ml. Passages 2 through 8 were used for the *in vivo* studies. Adherent choroidal and glioma cells were propagated by diluting trypsin-treated cells 1:10 in medium when at 80% confluence.

DEVELOPMENT OF INTRAOCULAR TUMORS: Adult transgenic Rag-2 "knockout" immunodeficient mice (15) were used for the study. Animals were handled at all times following the Association for Research in Vision and Ophthalmology Statement of the Use of Animals in Ophthalmology and Vision Research. The right eyes of mice were injected with either Y79 or WERI-Rb human retinoblastoma cells. Each animal was first anesthetized with an intraperitoneal injection of 20-30 μl of sodium pentobarbital (Nembutal) solution, 50 mg/ml. The pupil was then dilated with 2-3 drops of 2.5% phenylephrine hydrochloride solution and a drop of topical anesthetic proparacaine hydrochloride (0.5%) was applied. Cellulose eye drops (2.5%) and a glass contact lens were applied to the cornea to aid visualization of

the surgical procedures. Injections were performed using a surgical microscope. The conjunctiva of the temporal area of the eye was dissected and an incision was made was made at the scleral sulcus with a #11 disposable scalpel. Two microliters of sterile phosphate buffered saline containing 2 X 10^4 cells were injected into the vitreal cavity through the scleral sulcus using a Hamilton syringe with a 33 gauge canula. Special care was taken to prevent lens damage or posterior retinal punctures. The animals were examined at 1 and 24 hours and then weekly after surgery. Clinical findings regarding the presence of tumor were recorded. After 14 days, animals from the Y79 and WERI-Rb groups were sacrificed weekly. Necropsies were performed on every animal. The brain, eyes, mediastinum, lungs, heart and liver were examined microscopically. The brain was serially cross-sectioned to obtain coronal sections from frontal to occipital lobes and cross sections of the cerebellum, medulla and spinal cord.

HISTOPATHOLOGY: After dissection, the organs were immediately fixed in 10% formalin. The tissues were processed and embedded in paraffin using conventional automated systems. The blocks were sectioned to obtain levels and serial sections 4-5 microns thick and stained with conventional hematoxylin-eosin (H&E). The slides were examined and scored in a blinded fashion.

BINDING OF RETINOBLASTOMA CELL LINES TO CHOROIDAL AND GLIOMA CELL LINES: Monkey choroid, human glioma, or human embryonic kidney cells (1 x 10^5) were plated in a six well microtiter plate and allowed to adhere overnight. Y79 or WERI-Rb

retinoblastoma cells (1 x 10^6) were washed in 2 ml PBS and pelleted by centrifugation. The cells were resuspended in 0.2 ml Trypsin-EDTA solution (0.25% trypsin and 1 mM EDTA, Gibco BRL) for the indicated time. The reaction was terminated by the addition of 2 ml culture media. Cells (0.2 ml or 1 x 10^5 cells) were then layered over the adherent choroid, glioma, or embryonic kidney cell cultures and incubated at 37° C in humidified air containing 5% CO_2 for 3 hours. The culture fluid was decanted and the culture washed twice by vigorous shaking with culture medium (0.2 ml) warmed to 37° C. The three aliquots were pooled and the cells counted using a hemacytometer.

RESULTS

Y79 HUMAN RETINOBLASTOMA TUMORS: A total of 24 mice received Y79 retinoblastoma cells. Systematic *in vivo* examination of the mice eyes using an operating microscope demonstrated that the tumors were first observed in the vitreal cavity at 14 days after injection of the cells. Small cortical cataracts were found in the lens of all mice in the study, however, the cataracts did not interfere with adequate evaluation of the vitreal tumors. By 35 days, the tumors had obliterated the anterior chamber with the appearance of a whitish focally neovascularized cornea. After 49 days, some eyes also showed proptosis. Contralateral eyes were unremarkable.

HISTOPATHOLOGIC FINDINGS:

Eyes: Serial sections and levels of the eyes were obtained to evaluate the extent of the tumor in a tridimensional manner. Early retinoblastomas (14 days after injection) showed vitreal tumors that were located in the posterior and mid- equatorial regions of the cavity (Figure 1A*a*). The tumors were composed of small to medium size cells with scanty cytoplasm, hyperchromatic nuclei, frequent mitoses and rare necrotic cells (Figure 1A*b*). No rosettes or fleurettes were present. These features are similar to those of a poorly differentiated human retinoblastoma. The site of injection was identified as a fibroblastic scar in the sclera with attached peripheral retina and an occasional small focal vitreal hemorrhage (data not shown). As the time between the tumor cell injection and the sacrifice of the mice lengthened, tumors were larger and invaded various ocular structures (Table 1). By 21 days, the tumor showed subretinal and focal retinal invasion. By 21-28 days, focal choroidal invasion was observed (Figure 1A*c*). By 35-42 days, retinoblastoma had invaded the choroid, retina, subretinal space, and optic nerve of most of the eyes studied (Figure 1A*d,e*). At this time the vitreal tumor showed foci of necrosis. The tumor was focally present in the anterior chamber by 49 days (Figure 1A*f*). Between days 35-49, the tumors showed involvement of the ocular coats with focal corneal ulceration and invasion of the sclera. The sclera showed invasion by the tumor primarily at the injection site and extraocular tumor was also seen at this area. At 9 weeks, 1 mouse had evidence of tumor invading the lens. Two of the contralateral eyes of animals with tumors involving the optic nerve showed perineural invasion

by retinoblastoma (Figure 1A*g*), however, no intraocular tumor was observed in any of the contralateral eyes.

Brain: Mice with early intraocular tumors without invasion of the subretinal space or optic nerve had no metastases to the brain. After 35 days, eight mice had either tumor cells in the sub-arachnoid space (Figure 1A*h*) or focal brain parenchyma invasion (Figure 1A*i*) by retinoblastoma (Table 1). The corresponding ocular tumors had involvement of at least the choroid and, in most cases, the optic nerve and extraocular structures.

Heart, Lung, Mediastinum, and Liver: There was no tumor involvement at these sites by microscopic examination. Some animals had mild chronic inflammatory infiltrates in the liver at the level of the portal triads with associated microvesicular steatosis. These changes had no relation to the extent of tumor progression of ocular retinoblastoma and thus is probably an unrelated event.

WERI-Rb Human Retinoblastoma Tumors: Twenty mice received intraocular injections of WERI-Rb cells and were followed in this arm of the study. Examination of mice showed small vitreal tumors, first noted at 14 days after injection, visible only under the operating microscope. The lens frequently had cataracts. There was tumor extension in the anterior chamber by 35 days. After this time point most of the eyes appeared to have extensive tumor involvement in the anterior segment.

HISTOPATHOLOGIC FINDINGS:

Eyes: Histologic examination of early tumors (14-21 days) showed scanty amounts of tumor cells present mostly in the posterior vitreous (Table 2, Figure 1B*a*). The tumor cells were small to medium in size with scanty cytoplasm and hyperchromatic nuclei. The cells grew in a trabecular pattern. No fleurettes or true rosettes were found (Figure 1B*b*). There were no areas of necrosis or calcification seen. By day 28, the tumor focally invaded the retina but rarely the subretinal space (Figure 1B*c*). In most of the cases with subretinal involvement, tumors were contiguous with the site of injection or were evident in advanced disease. In striking contrast to the Y79 retinoblastoma cells, WERI-Rb retinoblastoma cells were predisposed to invade the anterior uveal tissues (anterior choroid, ciliary body and iris), and lens (Figure 1B*d,e*). Tumor invasion of optic nerve (Figure 1B*f*) or brain (data not shown) was lacking in the WERI-Rb injected eyes. Extraocular extension was seen in advanced tumors and almost always through the injection site (data not shown).

Brain: There were no tumor cells found in the meninges or brain parenchyma in the WERI-Rb injected group.

Heart, Lung, Mediastinum, and Liver: No involvement of the heart, lung, mediastinum, or liver was observed. Inflammatory changes in the liver were similar to those seen in the Y79 injected group.

IN VITRO BINDING OF RETINOBLASTOMA CELL LINES TO CHOROIDAL AND GLIOMA CELL LINES

One contributing characteristic to the development of metastases is the specific trafficking of tumor cells to the target organ. To test the hypothesis that Y79 cells might metastasize by specifically adhering to choroidal or glial cells, suspensions of either Y79 or WERI-Rb cells were incubated with the adherent RF/6A monkey choroidal cell line. After one hour, non-adherent cells were removed by vigorous washing with media and the plates were observed under the microscope (Figure 2A). Plates containing Y79 cells showed a significant percentage of the retinoblastoma cells bound to the monkey choroidal cell line while plates containing WERI-Rb cells showed little binding. Similar results were found when the two retinoblastoma cell lines were incubated with the Hs 683 human glioma cell line (Figure 2A). Neither retinoblastoma cell line exhibited significant binding to the HEK293 human embryonic kidney cell line (Figure 2A). Trypsin treatment of Y79 cells reduced the binding of these cells to both the choroidal and glioma cell lines (Figure 2B) while similar treatment with neuraminidase had no effect on binding (data not shown). At each trypsin treatment time indicated, cells in the pooled supernatant and washes were counted on a hemacytometer. Figure 3 shows the trypsin-dependent reduction of Y79Rb cell binding to the choroid cells. Similar results were obtained when glioma cells were used as the test cells (data not shown).

DISCUSSION

Without an animal model of naturally occurring disease, advances in the study and the treatment of retinoblastoma have been difficult and have progressed only through the evaluation of the disease in infants and small children. Previous attempts to develop animal models of retinoblastoma have only been partially successful in mimicking the human disease.

The retinoblastoma tumors that develop after intraocular injections of Y79 human retinoblastoma cells into immunodeficient mice described in the present study closely resemble the tumors of metastatic human retinoblastoma. An intravitreal injection of Y79 retinoblastoma cells caused the initial formation of a small intravitreal tumor. Only minimal trauma to the lens, peripheral uvea and retina occurred. Tumors were then found to invade the subretinal and choroidal space followed by invasion of the optic nerve. Subsequently, the brain showed evidence of metastasis and finally the tumor involved the contralateral optic nerve. This tumor progression occurred over a relatively reproducible time span following the intravitreal injection of the Y79 retinoblastoma cells.

A parallel model was developed using intravitreal injections of an alternate human retinoblastoma cell line (WERI-Rb). The procedures were identical in all studies. A striking difference between the tumor models was documented. While both retinoblastoma cell lines developed into intraocular tumors that closely resembled human retinoblastoma, the WERI-Rb tumors exhibited characteristics of localized,

non-metastatic human retinoblastoma and the Y79 tumors exhibited the histopathologic characteristics of metastatic human retinoblastoma with invasion and colonization of the optic nerve and brain. One possible explanation for this observation is that the rates of growth of these cell lines are different. Thus, if the experimental animals in the WERI-Rb group were observed for a longer period of time, metastases to the posterior choroid or CNS axis might eventually be found. In fact, the rates of growth of the Y79 cells *in vitro* are more rapid than the WERI-Rb cells using the growth conditions described in these experiments. However, by the end of the experiment, the animals in both groups had tumors that had completely replaced the normal ocular tissues in the affected eye and the animals appeared to have discomfort. Allowing the animals to survive for a longer period of time was felt to be unethical. The Y79 animal model at the very least appeared to mimic the aggressive, rapidly growing, metastatic retinoblastomas only occasionally observed in North America and Europe but more commonly seen in Mexico, Central and South America, Saudi Arabia, and India. The WERI-Rb animal model behaved like patients with nonmetastatic retinoblastoma more commonly seen in Europe and North America. Therefore therapies for both observed types of retinoblastoma could be studied in these predictable animal models.

In vitro binding studies suggested that a specific difference in the membrane protein structure of the cells may at least in part play a role with the observed difference in metastatic behavior of the two animal models. Using adherent cell lines derived from monkey choroid and human glioma cells derived from tissues that are similar

in origin to the target tissues of metastatic retinoblastoma, Y79 cells were found to rapidly bind. Specificity was suggested since Y79 cells did not bind to human embryonic kidney cells. Trypsin abolished this binding suggesting protein on the surface of Y79 cells was apparently involved in the cell-cell interaction. WERI-Rb cells did not appear to interact with choroidal, glioma, or embryonic kidney cell lines under the same experimental conditions. Understanding the mechanism of this binding may aid in understanding the biochemical events that allow for metastasis of retinoblastoma. Furthermore, this simple *in vitro* binding assay may help predict which patients with retinoblastoma might be prone to develop metastases.

Distant metastases outside the central nervous system were not observed in these animal models. Metastases outside of the central nervous system in human disease is only rarely observed and is considered a very late event in the course of the disease. These distant metastases are felt to be derived from the vascular route probably seeded via choroidal invasion. Although choroidal invasion was eventually always observed in the Y79 cell animal model, the animals were not allowed to survive for a long period of time. If the animals were allowed to progress, it is possible that distant metastases outside of the central nervous system might have been observed.

All of the animal models described previously may have utility in particular research protocols but none is perfect in all settings. The prognosis of children with retinoblastoma depends on the finding of choroidal or optic nerve invasion at the

time of diagnosis (16). The models described in this paper provide an opportunity for research in the biological behavior and treatment of both metastatic and nonmetastatic retinoblastoma that closely mimic the appearance of human disease.

ACKNOWLEDGMENTS

We gratefully acknowledge the assistance and support of Dr. Milton Finegold, Department of Pathology, Baylor College of Medicine.

REFERENCE LIST

1. McClean I, Burnier M, Zimmerman L, Jakobiec F: *Tumors of the Retina.* Tumors of the eye and adnexa. Atlas of tumor pathology. Edited by Rosai J. Washington, D.C., Air Force Institute of Pathology, 1994, pp. 100-135

2. Eng C, Li FP, Abramson DH, Ellsworth RM, Wong FL, Goldman MB, Seddon J, Tarbell N, Boice JD Jr: Mortality from second tumors among long-term survivors of retinoblastoma. J Natl Cancer Inst 1993, 85:1121-1128

3. Advani SH, Rao SR, Iyer RS, Pai SK, Kurkure PA, Nair CN: Pilot study of sequential combination chemotherapy in advanced and recurrent retinoblastoma. Med Pediatr Oncol 1994, 22:125-128

4. Byrne J, Fears TR, Whitney C, Parry DM: Survival after retinoblastoma: long-term consequences and family history of cancer. Med Pediatric Oncol 1995, 24:160-165

5. Kaste SC, Chen G, Fontanesi J, Crom DB, Pratt CB: Orbital development in long-term survivors of retinoblastoma. J Clin Oncol 1997, 15:1183-1189

6. al-Ubaidi MR, Font RL, Quiambao AB, Keener MJ, Liou GI, Overbeek PA, Baehr W: Bilateral retinal and brain tumors in transgenic mice expressing simian virus 40 large T antigen under control of the human interphotoreceptor retinoid-binding protein promoter. J Cell Biol 1992, 119:1681-1687

7. Howes KA, Lasudry JGH, Albert DM, Windle JJ: Photoreceptor cell tumors in transgenic mice. Invest Ophthalmol Visual Sci 1994, 35:342-351

8. Madreperla SA, Whittum-Hudson JA, Prendergast RA, Chen P-L, Lee W-H: Intraocular tumor suppression of retinoblastoma gene-reconstituted retinoblastoma cells. Cancer Research 1991, 51:6381-6384

9. Gallie BL, Albert DM, Wong JJ, Buyukmihci N, Pullafito CA: Heterotransplantation of retinoblastoma into the athymic "nude" mouse. Invest Ophthalmol Vis Sci 1977, 16:256-259

10. Kaufman PL: Aqueous Humor Dynamics. Duane's Clinical Ophthalmology Glaucoma. Edited by Parrish RK II. Philadelphia, J.B. Lippincott, 1992, pp 1-24

11. Sebag J: Vitreous Biochemistry, Morphology, and Clinical Examination. Duane's Clinical Ophthalmology Diseases of the Retina. Edited by Benson, WE. Philadelphia, J.B. Lippincott, 1992, pp 1-21

12. Rowe SG, Lee WH, Madreperla S: Subretinal and vitreal growth of human retinoblastoma cells in the mouse eye. Invest Ophthalmol Visual Sci 1992, 33:875

13. del Cerro M, Seigel GM, Lazar E, Grover D, del Cerro C, Brooks DH, DiLoreto D Jr, Chader G: Transplantation of Y79 cells into rat eyes: An *in*

vivo model of human retinoblastomas. Invest Ophthalmol Visual Sci 1993, 34:3336-3346

14. Albert DM, Griep AE, Lambert PF, Howes KA, Windle JJ, Lasudry JG: Transgenic models of retinoblastoma: What they tell us about its cause and treatment. Trans Am Acad Opthalmol Soc 1994, 92:385-401

15. Shinkai Y, Rathbun G, Lam KP, Oltz EM, Stewart V, Mendelsohn M, Charron J, Datta M, Young F, Stall AM, Alt FW: RAG-2 deficient mice lack mature lymphocytes owing to inability to initiate V(D)J rearrangement. Cell 1992, 68:855-867

16. Shields JA: The expanding role of laser photocoagulation for intraocular tumors. The1993 H. Christian Zweng Memorial Lecture. Retina 1994, 14:310-322

Site / Weeks	2	3	4	5	6	7	8	9
vitreous	+ 2/3	+3/3	+3/3	+3/3	+6/6	+3/3	+2/2	+1/1
retina		+2/3	+2/3	+3/3	+6/6	+3/3	+2/2	+1/1
subretinal space		+2/3	+2/3	+3/3	+6/6	+3/3	+2/2	+1/1
iris							+1/2	+1/1
lens								+1/1
anterior chamber						+1/3	+2/2	+1/1
choroid			+1/3	+3/3	+4/6	+3/3	+2/2	+1/1
optic nerve				+1/3	+3/6	+2/3	+2/2	+1/1
extra-ocular							+1/2	+1/1
brain				+2/3	+4/6	+1/3	+2/2	+1/1
contralateral eye							+1/2	+1/1

Table 1. Tumor progression of Y79 retinoblastoma injected mice. Mice were autopsied and the tissues examined histologically as described in Methods. The data are expressed as the number of animals that were positive for tumor at each site/total number of animals examined. Empty cells represent tissues without evidence of tumor in any of the examined animals.

Site / Weeks	2	3	4	5	6	7	8	9
vitreous	+ 2/2	+2/2	+2/2	+2/2	+4/4	+5/5	+2/2	+1/1
retina			+1/2	+2/2	+4/4	+5/5	+2/2	+1/1
subretinal space					+3/4	+4/5	+2/2	+1/1
Iris				+2/2	+2/4	+4/5	+2/2	+1/1
Lens				+1/2	+2/4	+2/5	+1/2	+1/1
Anterior chamber				+1/2	+2/4	+4/5	+2/2	+1/1
Choroid					+3/4	+3/5	+2/2	+1/1
Optic nerve								
Extraocular							+1/2	+1/1
Brain								
Contralateral eye								

Table 2: Tumor progression of WERI-Rb retinoblastoma injected mice. Mice were autopsied and the tissues examined histologically as described in Methods. The data are expressed as the number of animals that were positive for tumor at each site/total number of animals examined. Empty cells represent tissues without evidence of tumor in any of the examined animals.

Figure Legends

Figure 1A. Histology of Y79 *retinoblastoma mouse model.* Y79 retinoblastoma cells (2×10^4) were injected into the vitreal space of transgenic Rag-2 "knockout" immunodeficient mice. Tissues were histologically examined at the indicated days post-injection as described in Methods. ***a***, Eye at 14 days with a tumor (➔) in the vitreal cavity (Vi), normal lens (L) and retina (R). 40X ***b***, Tumor in the vitreal space showing small to medium size cells with scanty cytoplasm, hyperchromatic nuclei, and frequent mitoses. 400X ***c***, Eye at 21 days showing lens (L), retina (R), tumor in the vitreous (➔), and tumor invasion of the choroid (↑). 40X ***d***, Eye at 42 days showing tumor (➔) in the vitreal space (Vi) with an area of necrosis (⇒), tumor invading the choroid (C), retina (R), and subretinal space (SR). 40X ***e***, Eye at 42 days showing tumor (➔) in the subretinal space and tumor (➔) invading the optic nerve (ON). 40X ***f***, Eye at 49 days showing normal lens (L) with tumor (➔) in the anterior chamber (AC). 40X ***g***, Contralateral eye at 56 days showing normal retina (R) and tumor (➔) invading the optic nerve (ON). 40X ***h***, Brain (B) at 42 days showing tumor (➔) in the ventricular space (V). 40X ***i***, Optic chiasm (OC) at 42 days showing tumor (➔) invasion of the neural tissue. 100X.

Figure 1B. Histology of WERI-Rb retinoblastoma mouse model. WERI-Rb cells (2×10^4) were injected into the vitreal space of transgenic Rag-2 "knockout" immunodeficient mice. Tissues were histologically examined at the indicated days post-injection as described in Methods. ***a***, Eye at 14 days with normal retina (R),

lens (L), and optic nerve (ON) with a small tumor (→) in the vitreal space. 40X ***b***, Tumor (→) showing small to medium size cells with scanty cytoplasm and hyperchromatic nuclei. 400X ***c***, Eye at 28 days with normal lens and tumor (→) in the vitreal space exhibiting minimal invasion (→) of the retina (R) and ciliary body (CB). 40X ***d***, Eye at 42 days with large tumor in the vitreal space invading (→) the lens (L). 40X ***e***, Eye at 42 days with large tumor (→) invading the choroid (C), ciliary body (CB), and iris (I). 100X ***f***, Eye at 42 days showing large tumor (→) in the vitreal space adjacent to a normal retina (R) and optic nerve (ON) free of tumor. 40X

Figure 2. Binding of suspended retinoblastoma cells to adherent choroidal and glioma cells. A. Y79Rb (a, b, c) or WERI Rb (d, e, f) cells were suspended over adherent monkey choroid (a, d), human glioma (b, e), or human embryonic kidney (c, f) cells as described in Methods. (200X). B. Y79Rb cells were pretreated without (a, c) or with (b, d) trypsin for 5 minutes. The cells were suspended over adherent choroid (a, b) or glioma (c, d) cells for 3 hours as described in Methods. (200X).

Figure 3. Trypsin treatment of retinoblastoma cells abolishes binding to adherent choroidal cells. Y79Rb cells were treated with trypsin for the indicated time as described in Methods. The cells were suspended over adherent cells for 3 hours and washed. The cells in the pooled washes were counted on a hemacytometer.

A

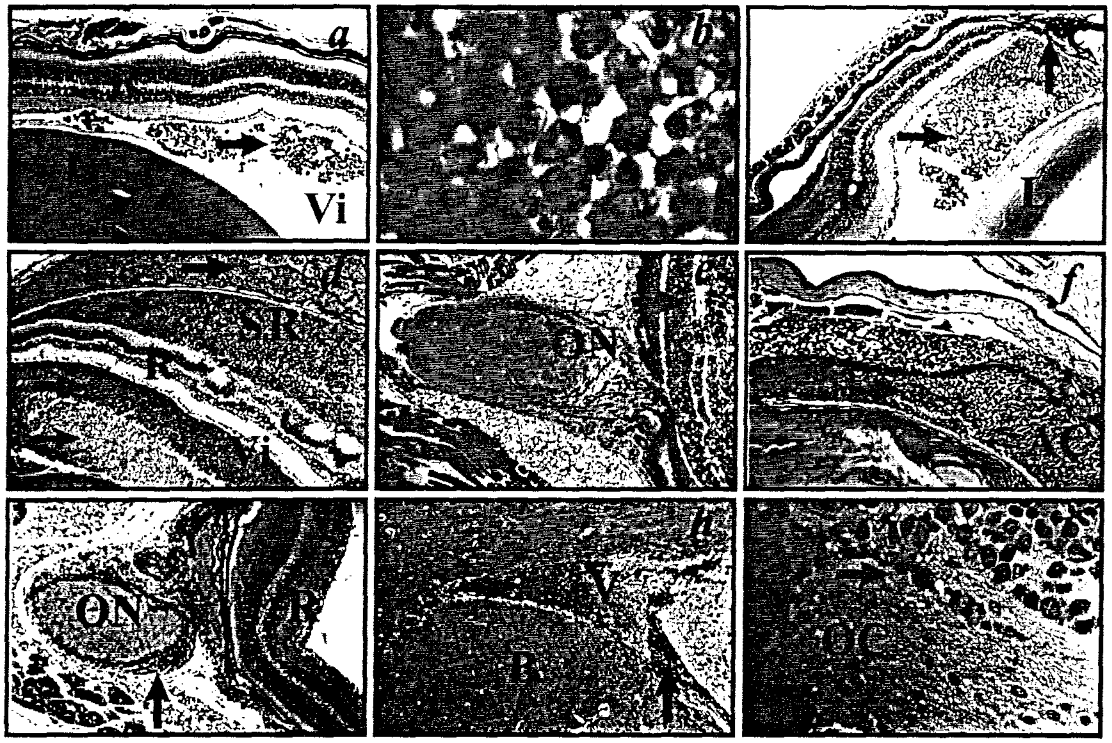

B

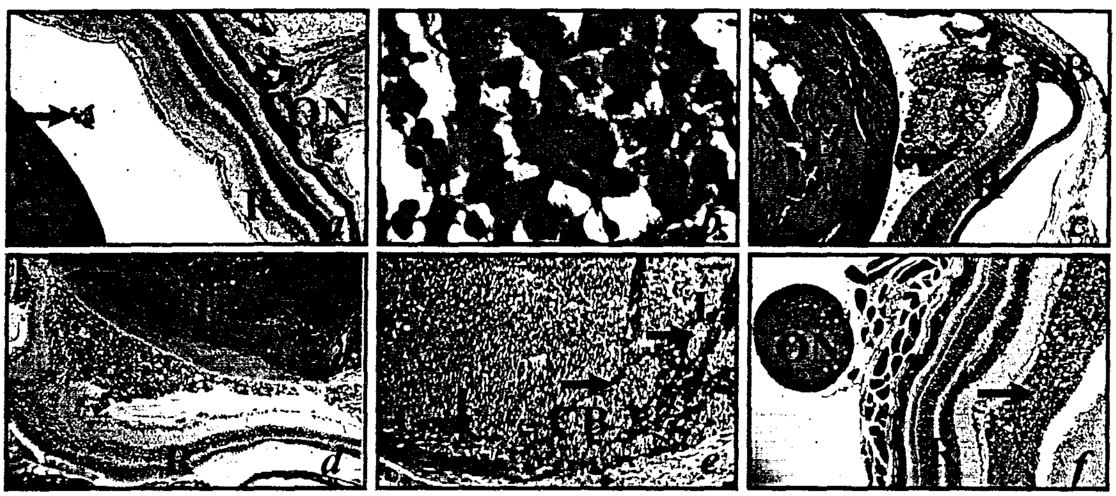

A

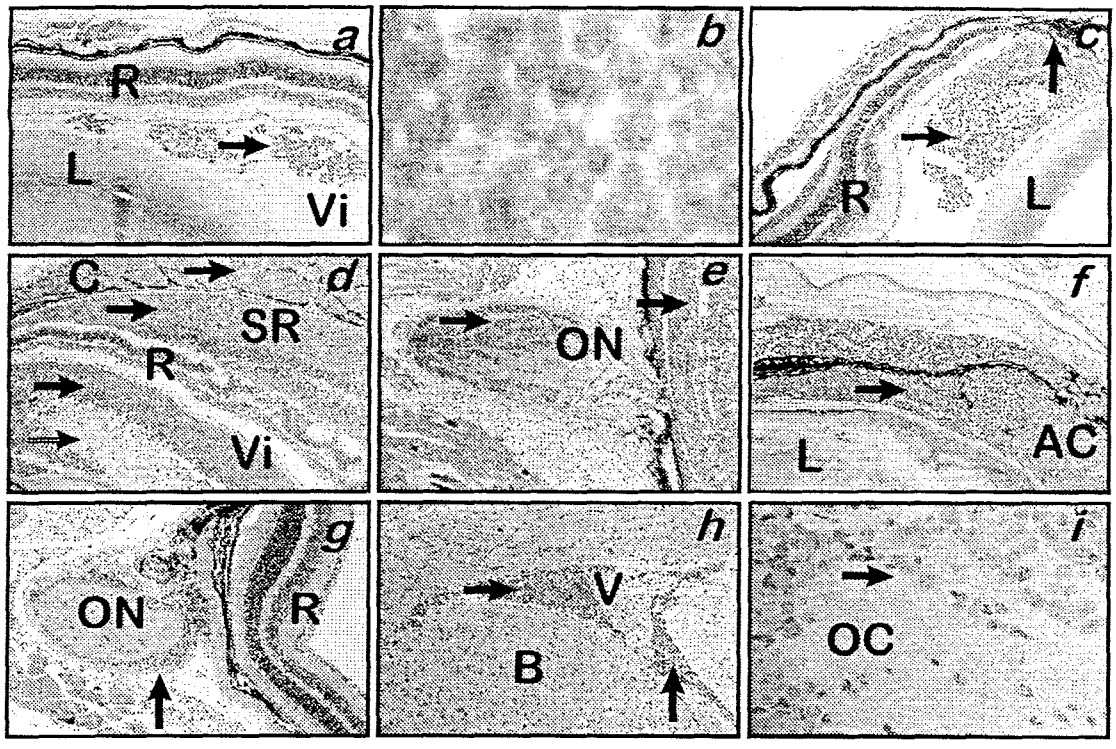
a
R
L
Vi
b
c
R
L
C
d
SR
R
Vi
e
ON
L
f
L
AC
g
ON
R
h
V
B
i
OC

B

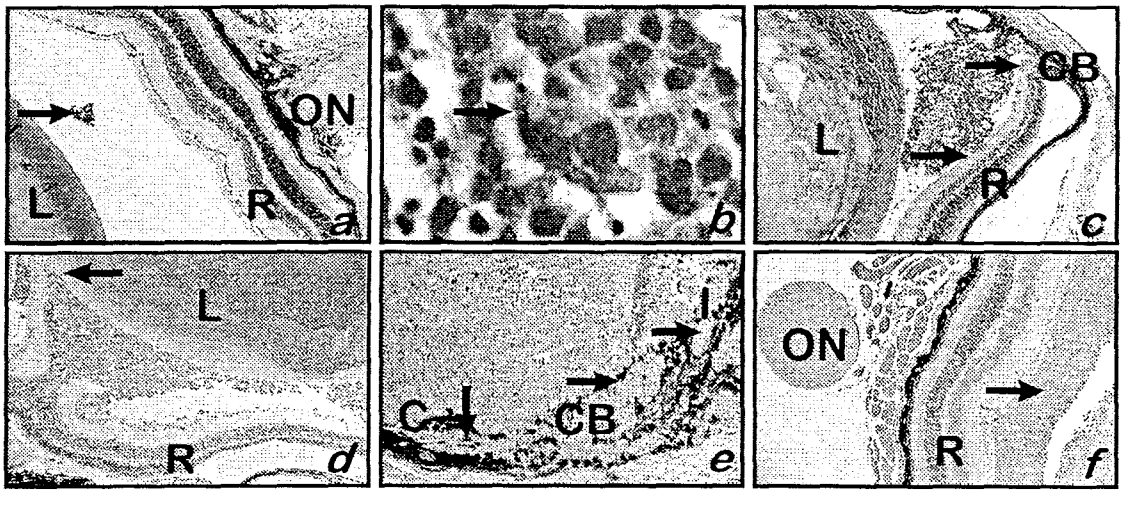
ON
L
R
a
b
CB
L
R
c
L
R
d
C
CB
e
ON
R
f

A

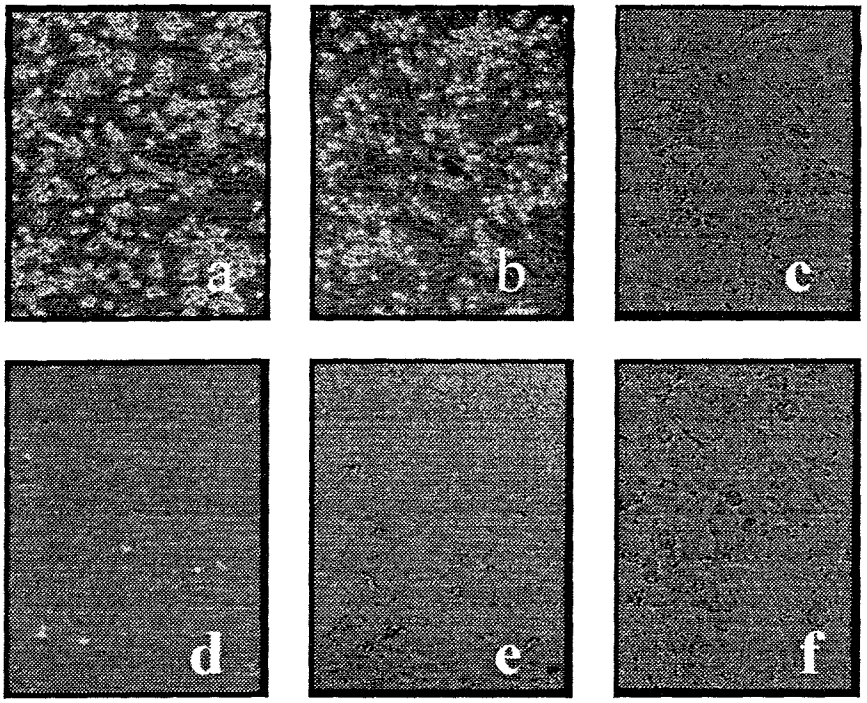

B

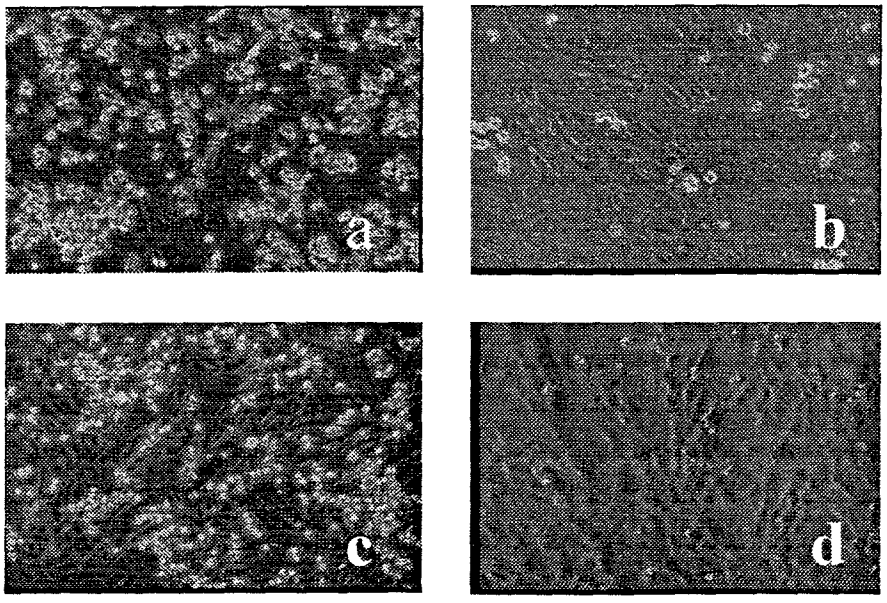

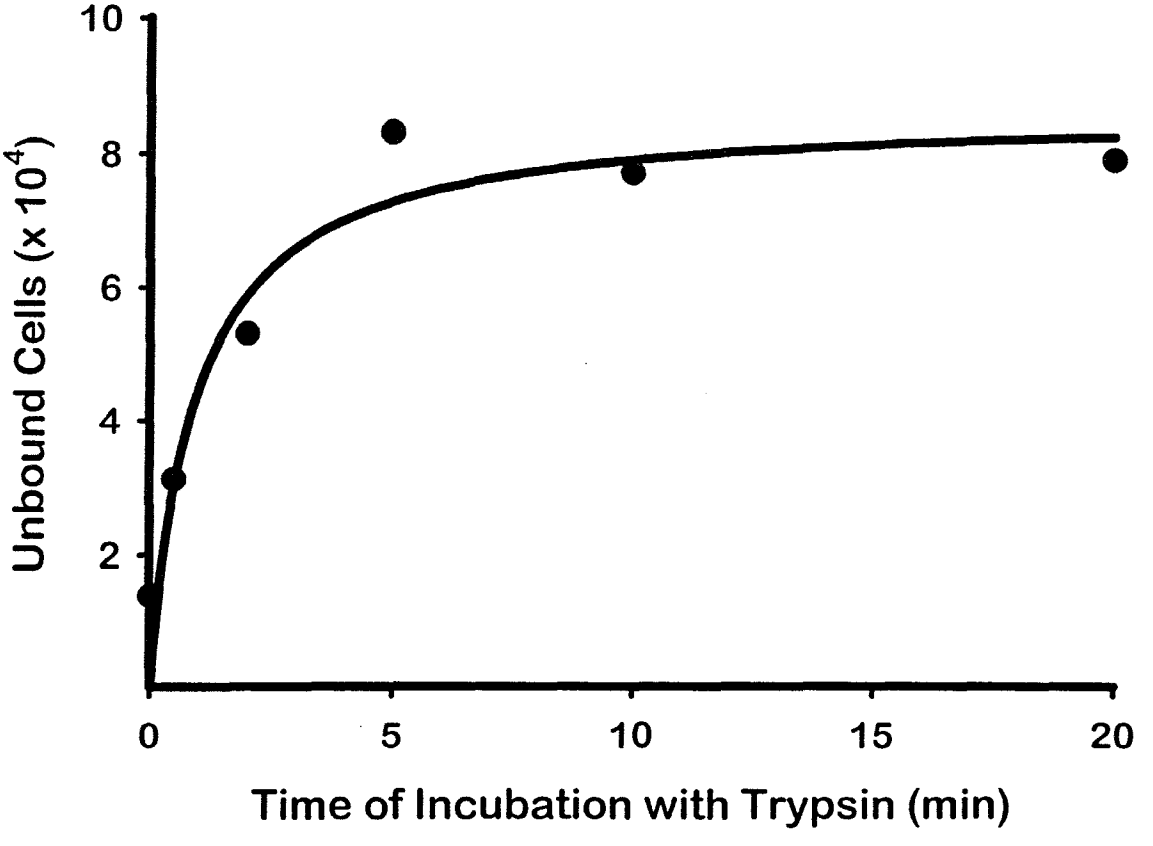
10
8
6
4
2
Unbound Cells (x 10^4)
0
5
10
15
20
Time of Incubation with Trypsin (min)